Effects on Interfacial Properties and Cell Adhesion of Surface Modification by Pectic Hairy Regions

Marco Morra,* Clara Cassinelli, and Giovanna Cascardo

Nobil Bio Ricerche, Str. S. Rocco 36, 14018 Villafranca d'Asti, Italy

Marie-Danielle Nagel

Université de Technologie de Compiègne, UMR 6600 Domaine Biomatériaux-Biocompatibilité, Centre de Recherches de Royallieu, Compiègne, France

Claudio Della Volpe, Stefano Siboni, Devid Maniglio, and Marco Brugnara

Department of Materials Engineering and Industrial Technologies, University of Trento, Trento, Italy

Giacomo Ceccone

Institute for Health and Consumer Protection, European Commission Joint Research Center, Ispra, Italy

Henk A. Schols

Laboratory of Food Chemistry, Wageningen University, Wageningen, The Netherlands

Peter Ulvskov

Biotechnology Group, Danish Institute of Agricultural Sciences Frederiksberg, Denmark

Polystyrene Petri dishes, aminated by a plasma deposition process, were surface modified by the covalent linking of two different enzymatically modified hairy regions (HRs) from pectin containing, for example, rhamnogalacturonan-I and xylogalacturonan structural elements. The two polysaccharide preparations share the same structural elements of apple pectin, but the relative amounts and lengths of the neutral side chains present differ. Surface analysis by X-ray photoelectron spectroscopy, contact angle measurement, and atomic force microscope (AFM) force−separation curves was used to characterize the effects on surface chemistry and interfacial forces of the surface modification process. Cell adhesion experiments using continuous L-929 fibroblasts and primary aortic smooth muscle cells were performed to evaluate the effect of the polysaccharide nature on cell adhesion. Results show that immobilization of the HR affects the interfacial field of forces and the cell behavior: "equilibrium" contact angles, obtained by a recently introduced vibrational approach, decrease after HR immobilization reaching a value close to 20°. AFM force−separation curves show a more extended (or softer) interface in the case of the HR bearing longer side chains. Accordingly, depending on the HR preparation, cells shifted from spread morphology and adhesion behavior quantitatively comparable to that observed on conventional tissue culture polystyrene to rounded morphology and significantly lower adhesion. These data show that engineering of plant pectins can be a valuable tool to prepare novel and finely tuned polysaccharides having different chemico-physical and biological properties, to be used in the surface modification of medical devices and materials.

Surface modification of medical materials and devices by polysaccharides is presently a topic of great interest, both at a fundamental and applied level.[1,2] Recent literature actually shows that this field is undergoing significant advancement and evolution. Except for heparin, whose widespread use as a coating in blood-contacting devices exploits a specific interaction,[3−6] hydrophilic polysaccharides, such as dextran, have long been used as "bio-passive" materials, because of their extensive hydration and low protein adsorption properties.[7,9] Naturally occurring alginate and hyaluronan have been used mostly because of their favorable physical properties, primarily extensive hydration, in wound healing and post-surgery applications.[10−12] Contrary to this biopassive scenario, recent advancements stress the biological and bioactive
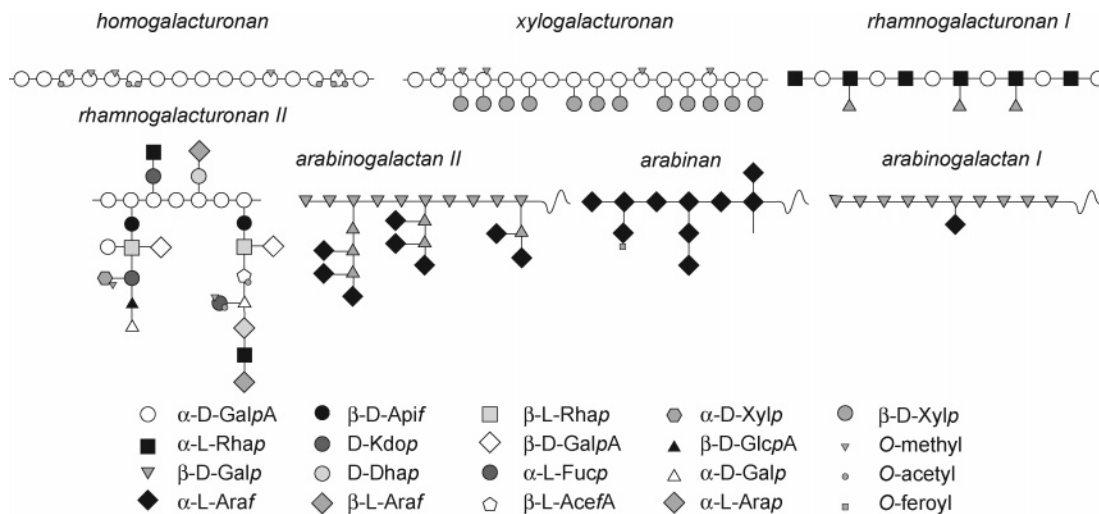
Figure 1. Structural elements of pectins.[17]

role of polysaccharides and the largely untapped opportunities lying in the full understanding and exploitation of their cell-signaling properties.[13,14] Thus, it was recently shown that alginate did not owe its success as a wound dressing material to a simple "moist-healing" mechanism[15] but to the bio-active effect it exerts on macrophages.[16] As to hyaluronan, once just considered a highly hydrated random coil, it is more and more discussed in terms of its intrinsic bioactivity and specific interaction with cell surface receptors.[10–14] In short, there is an increasing trend toward focusing on the more sophisticated biological properties of the polysaccharides rather than solely on their physical properties.[13,14]

In light of the previous comments, pectic polysaccharides, present in most plant tissues, represent an untapped resource and an interesting area of investigation. Pectin is reported to consist of many different structural elements[17] as is visualized in Figure 1. The precise structure and relative amounts of these structural elements differ among plant species and the type of tissue. Next to homogalacturonan (smooth regions) consisting of galacturonic acid sequences partly esterified with methanol at C-6, rhamnogalacturonan-I (RG-I) is the most abundantly present subunit in the so-called hairy regions (HRs) or ramified regions of pectin. RG-I is built from a backbone of sequences of alternating rhamnose and galacturonic acid residues,[18,19] while arabinan and (arabino-)galactan side chains may be present at O-4 of (some of) the rhamnosyl residues. Acetyl groups may be present on galacturonic acid residues in RG-I as well; to date, no evidence is present that the galacturonic acids in RG-I are methyl esterified. Other structural elements of pectin are xylogalacturonans (partly methyl esterified galacturonans with some of the galacturonic acid residues substituted at O-3 with beta-linked xylose)[17,20] and finally a very complex rhamnogalacturonan-II segment, which is rather well conserved across plant families[17,18](see Figure 1). The relative amounts of the various segments and their precise chemical fine structures [molecular weight (MW), total charge, level of branching] determine the physicochemical properties of the polysaccharide.[17] In previous pectin models,[21] homogalacturonans are interdispersed with segments of RG-I backbone. Recently, indications are presented that galactu-

ronan chains are side chains attached to the RG-I backbone.[22] Importantly, biotechnological techniques are being developed for the *in planta* engineering of rhamnogalacturonan side chains structures,[23,24] and techniques for tailoring side chain structures in vitro by specific enzymes are well established as visualized in Figure 2 for the "old" model (Figure 2). Because the enzymes are specific for the individual structural pectic elements, their actions do not depend on the overall architecture of the pectins.[21,25] This way, it is possible to obtain modified pectic polymers, enriched in, for example, rhamnogalacturonans decorated with or without side chains. A simple procedure to isolate RG-I enriched fractions on a semi-large scale is to use commercial pectinase preparations to liquefy the tissue of fruits or vegetables.[25,26] The enzymes degrade the homogalacturonan part (smooth regions) of the pectin present and releasing the so-called HRs.

These pectic HRs form a natural choice for the control of hydration, because this is one of their roles in the plant cell walls.[17–19,22] Pectic polysaccharides isolated from various sources have been shown to exhibit effects on the human immune system. The possible mechanisms of action include influence on the complement cascade, endocrinal functions, and cytokine induction and the effect on chemotaxis of leucocytes.[27] Pectic polysaccharides from some plant species have recently been shown to contain RG-I fragments that have anti-ulcer and mitogenic activities and IL-6 enhancing activities.[28] Cell—cell interactions rely on displayed carbohydrate moieties and on sugar epitope specific binding proteins, for example, members of the galectin and selectin gene families. Metastasis of some cancers depends on the cancer cells' specific recognition of galactoside epitopes, a recognition that can be inhibited by appropriately engineered rhamnogalacturonans.[29]

On the basis of the previous considerations, the various structural elements of pectin could be of great potential interest in the surface modification of medical devices because they are polymers with negatively charged segments, while the polarity can be affected by controlling the length of the side chains. Furthermore, the methyl esterification present in native pectins (partly neutralizing the charges present) can be easily removed by alkali or enzymes to
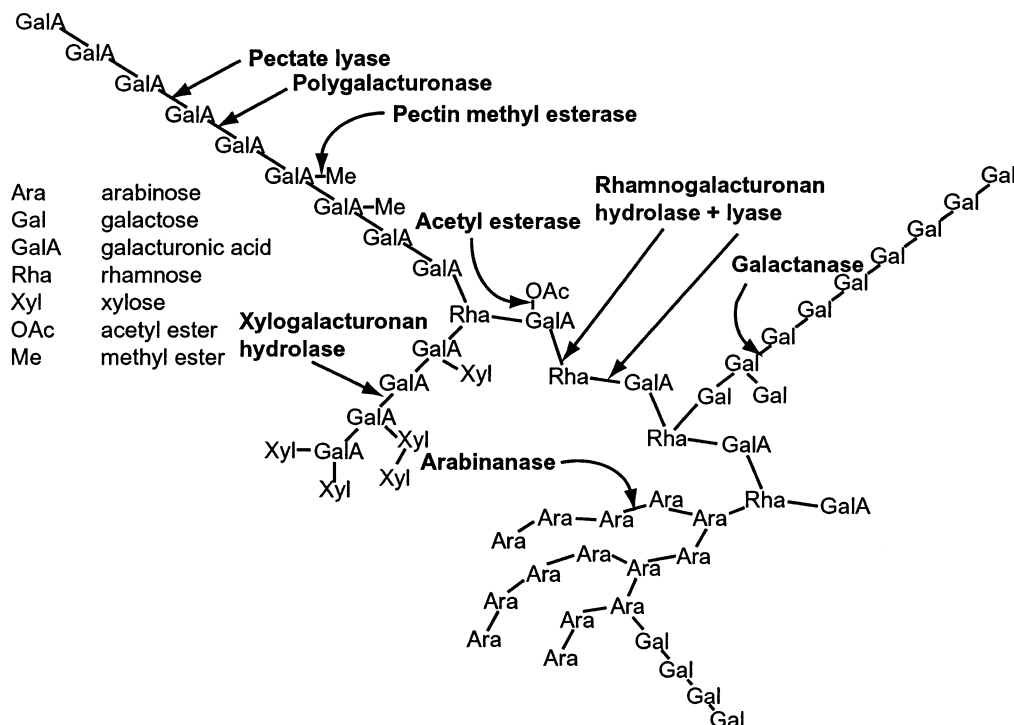
Figure 2. Sites of attack of enzymes able to modify the homogalacturonan and rhamnogalacturonan structural elements of pectins.[19]

vary the total charge present on the molecule. Also the acetyl substitution of the RG-I segments will make the rather hydrophilic molecule slightly more hydrophobic. The general RG-I structure permits, in many cases, oriented immobilization of the rhamnogalacturonan backbone bearing side chains of controllable length and nature, affecting interfacial hydration and possibly showing bioactive properties. The use of precision-engineered polysaccharides can allow defining the molecular structure−function relationships vital for the rational design of derivatized surfaces.

This paper presents the results of a multi-disciplinary effort aimed at producing a proof of concept of the use of pectic polysaccharides for the surface modification of medical devices. Briefly, two different modified hairy regions (MHRs) were obtained by enzymatic treatment of apple tissue. Both polysaccharide preparations were covalently coupled to polystyrene (PS) surfaces aminated by a plasma-deposition process; treated surfaces were characterized by surface-sensitive techniques such as X-ray photoelectron spectroscopy (XPS), contact angle measurement, and atomic force microscope (AFM) force−separation curves in aqueous solution. A continuous (mouse L-929 fibroblasts) and a primary (human smooth muscle cells, SMCs) cell line was used to evaluate the effect of the obtained surface chemistries on in vitro cell adhesion.

Experimental Section

Materials. Preparation of the two different MHRs was performed as described by Schols et al.[26] Homogenized apple tissue was treated with commercial enzyme preparations, and the resulting suspension was centrifuged. The juice was ultrafiltrated, and the ultrafiltration retentate was lyophilized to yield the MHR. MHR A was prepared by using the experimental enzyme preparation Rapidase C600, while MHR B was made by the use of Rapidase Liq+. Both enzymes were from DSM Food Specialities, Delft, The Netherlands. Characterization of the polymers was performed as described;[25,26] high-performance size-exclusion chromatography (HPSEC) was performed on three TosoHaas TSK-Gel G columns in series (4000PWXL−3000PWXL−2500PWXL) using 0.2 M sodium nitrate as the eluent; pectins were used to calibrate the system. Attenuated total reflectance infrared (ATR-IR) spectra of films obtained from aqueous solutions were obtained by a Mattson Research Series IR spectrometer, equipped with a 45° ZnSe crystal.

All chemicals used in surface modification (see below) were from Sigma Aldrich.

Surface Modification. Surface modification of PS Petri dishes was obtained as follows: PS was first surface-functionalized by the introduction of amino groups via deposition from allylamine plasma. Briefly, allylamine vapor was introduced from a reservoir kept at room temperature (RT) into a stainless steel, capacitively coupled parallel-plate reactor. The reactor is equipped with a radio frequency generator (13.56 MHz) and internal electrodes. The volume of the reactor chamber is about 3 dm³, and the distance between the electrodes 10 cm. The monomer flow rate, as evaluated by the increase of the pressure with the pump turned off, is about 50 sccm (standard cubic centimeters per minute). The pressure, before switching on the discharge, was 200 mTorr. The samples were located on the water-cooled grounded electrode, and deposition, using a discharge power of 100 W, was performed for 30 s, using a pulsed plasma with a duty cycle of 4 ms on and 4 ms off. After treatment and prolonged rinsing in doubly distilled water, samples were dried under a laminar flow hood. Aminated Petri dishes will be coded PSAm in the rest of the paper.

In the second step, MHR A or MHR B was covalently coupled to the surface amino groups on PS. In brief, 5 mL of an unbuffered 0.5% solution of either MHR A or MHR B was placed into the PSAm and coupled by carbodiimide-mediated condensation between carboxyl groups present in the MHR and amino groups of the surface. In particular, 0.04 g of dimethylaminopropylethylcarbodiimide hydrochloride (Fluka) and 0.03 g of *N*-hydroxysuccinimide (Fluka) were dissolved in the 5 mL of aqueous MHR solution. The reaction was carried on at RT overnight, and then samples were extensively rinsed in deionized water. Samples were dried under a laminar flow hood before cell adhesion experiments and surface characterization. Samples obtained by the linking of the two different sugars will be coded PSMHR B or PSMHR A, respectively.

Surface Characterization. *XPS.* XPS analysis was performed with a Perkin-Elmer PHI 5500 ESCA system. The instrument is equipped with a monochromatic X-ray source (Al Kα anode) operating at 14 kV and 250 W. The diameter of the analyzed spot is approximately 400 μm, the base pressure is 10^{-8} Pa. The angle between the electron analyzer and the sample surface was 45°. Quantification of elements was accomplished using the software and sensitivity factors supplied by the manufacturer.

Contact Angle Measurement. Contact angle measurements were performed using the sessile method by an autodeveloped goniometer, at RT; drops images were collected by a digital photo camera and analyzed by using a curve fitting method and the tangent approximation. A vibrational method, already presented for the Wilhelmy plate approach, has been adapted to the sessile method to obtain a "stable-equilibrium" profile of the meniscus drop. Full descriptions of the principles of the technique have been presented in previous papers.[30-32] Advancing and receding values were collected using the tilting plate method on the same apparatus. A precision of $1-2°$ is commonly obtained in normal conditions. Lower precision should be justified.

Each datum shown in Table 3 is the mean value of at least three different results. Water was freshly produced through a Milli-Q device.

The size of the sessile drops was in each case 3 μL, while the tilting plate drops had a volume between 8 and 10 μL. The frequency used for vibrational equilibrium ranged between 130 and 200 Hz, but in some cases a higher frequency (untill 450 Hz) was used to show the irreversible effect of the water contact on the analyzed surfaces. The obtained contact angles were evaluated by ANOVA, *t*-student test.

AFM Force versus Separation Curves. All measurements were performed with a NT-MDT Solver P47H AFM (NT-MDT Co., Moscow, Russia), using a V-shaped silicon nitride cantilever (200 μm length, spring constant, as indicated by the supplier, 0.06 N/m).

Force−distance curves were acquired in 0.0005 M NaCl solution. Briefly, an image of 7×7 μm was obtained and a 6×6 points grid was traced on the field of view, using the relevant software supplied by the producer. Force−distance curves were acquired in each of the 36 spots defined in this way. This procedure was repeated twice, in two different

areas, for each sample, to obtain a total of 72 curves for each sample in each solution.

In the force measurement, the sample was moved continuously up and down. Deflection of the cantilever and height position of the sample were recorded. The force was obtained by multiplying the deflection of the cantilever times its spring constant. In this case, the spring constant was not measured and the value suggested by the producer was used, but this does not affect the meaning of the data. Measurements were repeated using the same cantilever for the whole set of samples and repeated to confirm that the obtained values were not affected by wear or other unexpected effects on the tip. Differences between the data obtained on the same sample at different times were not significant, and the same general trend among different samples was detected.

To obtain force versus separation curves, the deflection of the cantilever must be subtracted to the piezo scanner position. The point of zero separation was determined from the linear part of the contact line.

Cell Adhesion Assay. To evaluate the effect of the different natures of the polysaccharides on cell adhesion and proliferation, short-term experiments were performed as follows. First of all, to check the generality of the effect, two widely different cell lines were used: continuous L-929 mouse fibroblasts and primary human aortic SMCs; details on culture conditions are reported below. The following experimental protocol was adopted: cells were seeded at a given density on tissue culture polystyrene (TCPS, control), PSAm, PSMHR B, and PSMHR A surfaces. Cell morphology was estimated by direct observation under an inverted microscope at 3 and 24 h, while cell adhesion was evaluated after 24 h of culture. In particular, for weak adhesion estimation, supernatants were collected, followed by two washes of the Petri dish, centrifugation, and pellet trypsination (to dissociate aggregates). Trypan blue exclusion test was performed to assess cell viability.

For the estimation of strong adhesion, trypsination of spread cells on the bottom of Petri dishes was performed, followed by two washes of the Petri dishes with serum. After centrifugation, trypan blue exclusion test was performed to evaluate cell count and viability. Percent cell proliferation was obtained by dividing the number of cells counted in weak and strong adhesion evaluation with the number of cells seeded at time 0. Percent cell adhesion and percent viability were obtained from cell counts and trypan blue exclusion tests.

For cell adhesion testing, samples were sterilized by treatment for 1 h with penicillin (200 units/mL) and streptomycin (200 μg/mL) and then washed three times before use.

L-929 Cell Culturing. Murine L929 fibroblasts (European Collection of Cell Culture, U.K.) were grown in minimum essential medium (Gibco BRL Life Technologies, Eragny, France), supplemented with 10% fetal bovine serum (FBS), penicillin (100 units/mL), streptomycin (100 μg/mL), and 1% 200 mM L-glutamine (Gibco BRL). Cells were grown in a 100% humidified incubator at 37 °C with 5% CO_2 and passaged $2-3$ days prior to use. They were seeded at 4×10^4 cells/cm² on control and experimental surfaces.
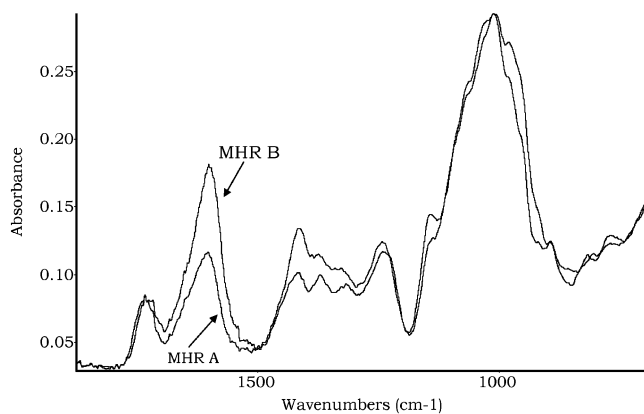
Figure 3. ATR-IR spectra of MHR B (grey) and MHR A (black) films obtained from aqueous solutions.

Table 1. Sugar Composition of Pectic HRs As Isolated from Apple Tissue Using Enzymes

sugar	MHR A	MHR B
rhamnose	5	11
arabinose	50	11
xylose	8	18
mannose	0	0
galactose	10	20
glucose	1	3
galacturonic acid	26	37
DM[a]	40	34
DAc[b]	55	11
% (w/w) sugar	66	78

[a] DM: mol methyl esters/100 mol of galacturonic acid. [b] DA: mol of acetyl groups/100 mol of galacturonic acid.

SMC Cell Culturing. Human umbilical artery SMCs (Cambrex Bio Science Milano Srl) were grown in smooth muscle basal medium supplemented with 5% FBS, 0.1% bovine insulin (5 mg/mL), 0.2% human fibroblast growth factor (1 μg/mL), 0.1% human epidermal growth factor (0.5 μg/mL), and 0.1% gentamicin sulfate + amphotericin B. Cells were grown in a 98% humidified incubator equilibrated with 5% CO_2 at 37 °C and subcultured before they reached 80% confluence. Cells were seeded at a density of 6 × 10^3 cells/cm^2 on control and experimental surfaces.

Data were analyzed using ANOVA and post hoc Tukey test (Instat software, GraphPad Software, Inc., San Diego, CA).

Results

Characterization of the Pectic HRs. ATR-IR spectra of films obtained from aqueous solutions of the two samples (Figure 3) show that, qualitatively, both polysaccharides share similar features: in particular, the —C=O stretching at 1740 cm^{-1}, the asymmetric stretching of carboxylate at about 1610 cm^{-1}, —CH$_2$ bending at 1425 cm^{-1}, and —C=O and C—O—C vibration at about 1077 and 1022 cm^{-1}, respectively.

Detailed characterization, as reported in the quoted refs 25 and 26, shows that the two preparations of modified pectic HRs differ significantly in their sugar composition as can be seen in Table 1. In MHR A, the side chains of RG-I are largely still present and are mainly composed of arabinose residues present in rather linear arabinan chains with a
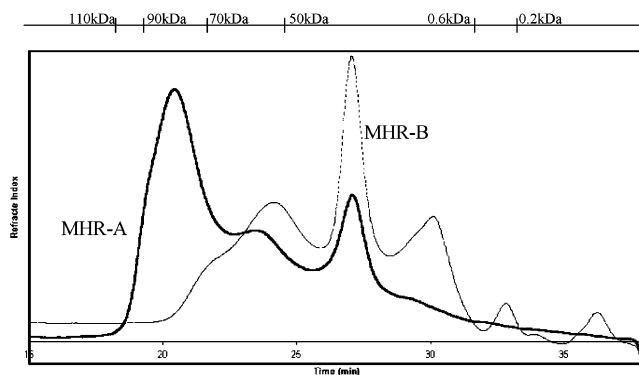

Figure 4. HPSEC of the two different pectic HR preparations. The patterns cover the MW range from 100 000 Da (20 min) to 200 Da (monomer galacturonic acid at 32.5 min).

Table 2. Surface Composition (atom %) As Detected by XPS Analysis of the Tested Samples

sample	C	O	N	other (less 1%)
untreated PS	100			
PSAm	79.2	4.5	16.3	
PSMHR B	70.4	22.6	6.5	S, Si, P
PSMHR A	68.1	25.0	6.3	Cl, S, Si, P

average length of more than 10 residues.[26] MHR B is prepared with an enzyme preparation rich in arabinan-degrading enzymes, and, consequently, the side chains have been removed quite effectively leaving 1—2 arabinose per side chain present on the rhamnose residues. The other sugars are enriched in the preparation, resulting in higher molar ratios. It is clear that the structural element xylogalacturonan is more dominantly present in MHR B. The galacturonic acid residues in MHR A are only partly methyl esterified (40%) while significant levels of acetyl groups are present (25 mol %). Especially the level of acetylation is much lower for MHR B (11%) as compared to that for MHR A (55%). HPSEC shows that both MHR preparations are rather polydisperse with respect to their MWs, covering the MW range from 100 000 Da to 200 Da, see Figure 4. Obviously, MHR B has a much lower average MW than MHR A. This is partly due to the removal of arabinose, although also some rhamnose—galacturonic acid linkages may be hydrolyzed by the enzyme rhamnogalacturonan hydrolase.[33] Although the two preparations are polydisperse in many respects (length of arabinan side chains, relative amount of xylogalacturonan, MW distribution) and the complete chemical structure is not completely resolved, we think that these preparations adequately illustrate the possibility of tailoring pectic molecules by enzymes.

XPS. Results of XPS analysis of untreated PS, PSAm, and PSMHR A or PSMHR B are reported in Table 2. Briefly, only carbon is detected on untreated PS (hydrogen is not detected in this kind of analysis), confirming the lack of contaminants and unexpected elements on the PS surface. After surface functionalization by deposition from allylamine plasma, significant amounts of nitrogen and oxygen were detected. Surface functionalization by the introduction of amino groups from allylamine plasma is well-known and widely exploited in surface modification by plasma.[34,35] The detected surface composition is, from a quantitative point of view, in agreement with published results. A pulsed

Table 3. Results of Water Contact Angle Measurements (Degrees)

sample	sessile angle	sessile (equilibrium) angle[a]	advancing angle	receding angle	contact angle hysteresis
PSMHR A	25 ± 1	21 ± 1[b]	37 ± 1	16 ± 1	21
PSMHR B	37 ± 2	32 (21)[b]	44 ± 4	21 ± 9	23
PSAm	37 ± 2	35 ± 1	43 ± 3	20 ± 2	23
TCPS	46 ± 1	35 ± 1	51 ± 4	30 ± 3	21

t-Student Probability for Groups of Data			
	TCPS	PSAm	PSMHR B
PSMHR A	different for all parameters	0.08 (adv)	0.2 (equ 450 Hz) 0.5 (rec)
PSMHR B		0.4 (sessile)	
	0.08 (adv)	0.8 (adv)	
	0.1 (rec)	0.85 (rec)	
PSAm	0.5 (equ)		
	0.06 (adv)		

[a] All "equilibrium" angles were obtained using a frequency ranging between 130 and 200 Hz. The bracketed value, in the PSMHR B line, was obtained using a vibrational frequency of 450 Hz, as reported in the experimental section. [b] On higher frequency vibrations the water drop is pushed downward, spreads, and irreversibly adheres to the polymer.

plasma was used in the present case, to avoid a too extensive disruption of the amino functionalities by plasma species, as well-known and reported.[36]

After polysaccharides coupling, a significant modification of the surface chemistry is detected: in both cases, the O/C ratio and the O/N ratio increase, as expected from the introduction of polysaccharides, which are characterized by a high oxygen-to-carbon ratio. Importantly, both surfaces show a significant amount of nitrogen, while no nitrogen is expected, and actually it is not detected, in the XPS analysis of powders of the two polysaccharides. This is in agreement with previous studies of surface immobilized polysaccharides such as alginate or hyaluronan:[8,37,38] because of the interfacial nature of the coupling reaction, the thickness of the surface polysaccharide layer is, broadly speaking, limited to a monomolecular layer, and it is thinner than the XPS sampling depth (<about 8 nm, at least in the ultrahigh vacuum environment of the chamber of analysis of the instrument). Thus, the detected surface stoichiometry arises from the convolution of the chemical composition of the surface polysaccharide layer and of the underlying aminated layer.[37]

The values observed are in general agreement with those obtained from other polysaccharide-coated surfaces. The C(1s) peak (not shown) was broadened following polysaccharide coupling with both samples, in agreement with the expected increase of chemical species bearing single and multiple C to O bonds.

Water Contact Angle Measurements. Results of contact angle measurement are reported in Table 3. In particular, the table shows, beside the commonly presented sessile, advancing and receding angles of water, the sessile equilibrium contact angle also, obtained by the input of vibrational energy to the sessile drop in contact with the surface.[30−32] The table reports also the results of statistical analysis by ANOVA. In particular, the lower part of the table shows the values of *t*-student probability for paired groups of data. The level of significance was taken below 0.05; that is, data

are considered significantly different if the *t* value is below 0.05. In the Table, *t* values are reported only if higher than 0.05, that is, only in the absence of a statistically significant difference.

Measurements were performed on PSAm, PSMHR A, and PSMHR B and on control TCPS. In the interpretation of the results, one should keep in mind the similar value of roughness of all the samples; given this reasonable hypothesis, all the differences come from the differences in chemical structure. The very similar values of the hysteresis correspond to a similar value of the chemical heterogeneity. All tested samples show relatively low advancing and receding angles, due to the high surface density of chemical moieties that can engage hydrogen bonding interactions with water. Within this general behavior, it is possible to detect a clear trend of contact angle values, in the order PSMHR A < PSMHR B < PSAm < TCPS. Surface hydrophilicity decreases in the same order; that is, the chemical structure appears to be more and more hydrophilic moving from the simply plasma-treated TCPS surface to the aminated surface and to the PSMHR B and PSMHR A surfaces. On the other hand, MHR compositions, as reported in Table 1, suggest that MHR B, because of the significantly lower acetylation and methyl esterification, is actually more hydrophilic than MHR A. This enhanced hydrophilicity of MHR B preparation is not reflected in wettability data likely for the two following reasons: part of the available carboxyl groups are probably involved in chemical bonding with the amino groups of the surface and do not contribute as ionic species to interfacial interactions with water; then, overall, the bulkier MHR A molecule yields a more hydrated, hydrogel-like interface (as also shown by AFM data in the section below), resulting in a lower contact angle as compared to that of PSMHR B. It is of interest to observe that conventional measurements (i.e., those obtained without the vibrational input), as reflected by the advancing, receding, and sessile contact angles, do not detect any significant difference between PSAm and PSMHR B. However, the very different nature of the surface structure is readily captured by vibrational evaluations: in the case of PSMHR B the standard deviation of the results is higher than in other cases and particularly the equilibrium value depends on the used frequency; at higher frequency the equilibrium value approaches the value of PSMHR A. A higher frequency, which is able to push the drop with an increased strength on the surface, irreversibly decreases the final contact angle of PSMHR B; this could be correlated to the possible dynamic properties of the surface, in the sense suggested by Andrade et al.[39] Once in contact with water, the initially less hydrophilic PSMHR B changes its conformation and becomes more similar to the more hydrophilic case (PSMHR A). However, a greater number of analyses and also the use of Wilhelmy method is necessary to confirm this hypothesis.

Statistical analysis of contact angle data allows an understanding of not only the limits but also the information contained in wettability results, particularly when using "vibrated" angles: differences between samples are not always significant. In particular, TCPS shows the same equilibrium and advancing angle as the aminated surface;
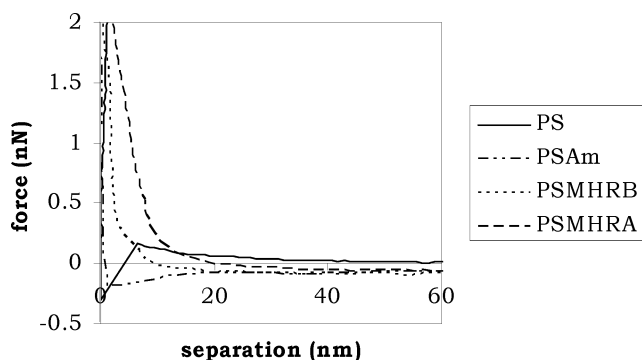
Figure 5. AFM force−separation curves obtained on approach in 0.0005 M NaCl.

this probably means that only the surface portion corresponding to the highest surface energy is different (receding angles). PSMHR B looks similar to TCPS for advancing and receding, but the difference is captured by the equilibrium angle; PSMHR B and PSAm yield similar values, except for the equilibrium angle, which once again is the only parameter able to capture the difference. As to comparison between PSMHR A and PSMHR B, the difference between the equilibrium angles disappears using high frequency of vibration or considering only the highest energy portion of the surface (receding). TCPS and PSMHR A is the only pair of samples that yields different results for each of the experimental data.

AFM Force−Separation Curves in Aqueous Solutions. AFM force−separation curves in aqueous solutions provide clear pictures of the interfacial field of forces at the AFM tip−sample interface and of how it was affected by the different surface chemistries probed in this work. In particular, Figure 5 shows the force−separation curves measured as the AFM tip approaches, in 5×10^{-4} M NaCl, the surfaces of untreated PS, PSAm, PSMHR B, and PSMHR A. In the case of untreated, hydrophobic PS, the curve shows a long-range repulsive (positive) force followed by a sudden jump-to contact, because of an attraction (negative) force. This behavior is typical of hydrophobic polymers in low ionic strength electrolyte solutions.[40] Basically, the long-range repulsive force is due to the electrostatic repulsion between the negatively charged PS and the cantilever tip surface. This is confirmed by the complete disappearance of this contribution in higher ionic strength solutions, because of the decrease of the Debye length and, hence, of the range of electrostatic repulsion. The detected jump to contact is the well-known, even if scarcely understood, outcome of interfacial interactions involving hydrophobic surfaces in aqueous environments, generally assigned to the so-called "hydrophobic force" or to the effect of nanosized air bubbles on the hydrophobic surface.[41−45] The discussion of this kind of force is outside the scope of the present paper; we just note that the observed curve is in agreement with the behavior expected on hydrophobic surfaces.

The force−separation curve obtained on the PSAm sample no longer shows the long-range repulsive force. Rather, the curve shows a long-range attraction (negative shift of curve) that culminates in a jump to contact. This behavior is consistent with the presence of positively charged amino
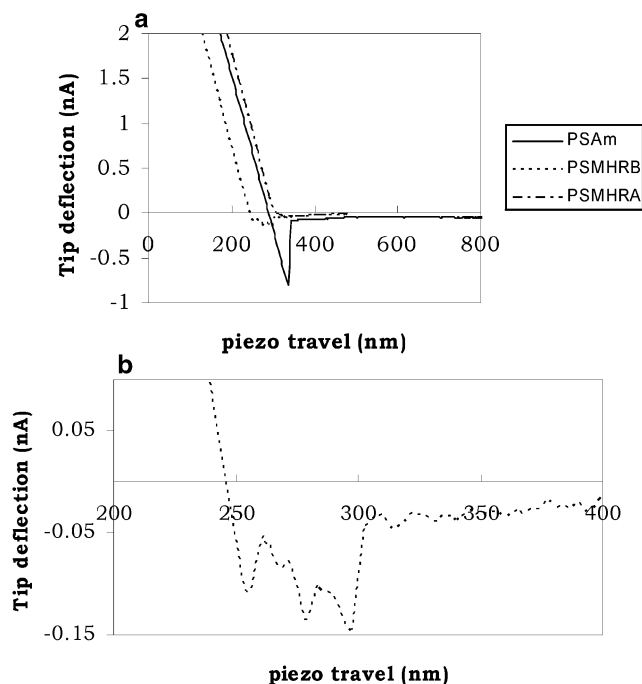

Figure 6. Tip deflection versus piezo travel of (a) retracting curves obtained by the AFM in 0.0005 M NaCl. (b) Detail of the retracting curve of PSMHR B.

groups on the PSAm surface and of an interfacial field of forces dominated by long-range electrostatic and short-range Lewis acid−base attraction between the positively charged (and electron acceptor) PSAm surface and the negatively charged (and electron donor) tip.

The immobilization of the short-haired, xylogalacturonan-enriched MHR B on the PSAm surface leads to significant modification of the interfacial field of forces: as shown in Figure 5, the force−separation curve does not show any attractive interaction until repulsive contact is reached. This is consistent with the introduction of hydrophilic, uncharged moieties on the sample surface, in agreement with XPS and contact angle data. Because of the hydrophilic nature of this surface, no driving force exists for the jump to contact typical of hydrophobic attraction; the neutralization of positively charged amino groups by the coupling reaction and ionic interaction between surface amino groups and carboxylate removes the source of attractive electrostatic interaction displayed by the PSAm sample. The curve detected at the PSMHR A−aqueous interface is generally similar to that of PSMHR B, the most significant difference being the longer range of the repulsive interaction. In the case of PSMHR A, the tip "feels" the repulsive presence of the surface at a distance of about 20 nm from contact. The most obvious source of this increased range of interaction is the bulkier nature and, hence, the increased span of steric interaction, promoted by the longer side chains of PSMHR A.

Interesting information was also obtained from the analysis of the curves detected upon tip retraction. Figure 6 compares retraction curves obtained at PSAm, PSMHR B, and PSMHR A 5×10^{-4} M NaCl interfaces. The figure shows the actual distance travelled by the piezo bearing the tip; that is, curves are not corrected for tip deflection as in the previous one. In Figure 6a, two extremes can be detected: detachment of the

Table 4. Results of Cell Adhesion and Proliferation Experiments: L-929 Cells

sample	viability of adherent cells (%)	viability of non- (or poorly) adherent cells	% adherent cells	proliferation
TCPS	99.33 ± 0.10	98.85 ± 0.29	96.28 ± 0.63	×2.5 ± 0.31
PSAm	99.15 ± 0.08	97.68 ± 0.23	98.16 ± 0.29	×2.4 ± 0.34
PSMHR B	98.85 ± 0.37	98.71 ± 0.85	97.16 ± 0.92	×2.5 ± 0.23
PSMHR A	99.42 ± 0.13	98.78 ± 0.34	6.0 ± 1.71[a]	×2.4 ± 0.13

[a] The differences between PSMHR A and PSMHR B, PSMHR A and PSAm, and PSMHR A and TCPS are statistically significant: $p < 0.001$. The differences between all other data are not statistically significant.

Table 5. Results of Cell Adhesion and Proliferation Experiments: SMC Cells

sample	viability of adherent cells (%)	viability of non- (or poorly) adherent cells	% adherent cells	proliferation
TCPS	99.48 ± 0.19	99.15 ± 0.25	96.92 ± 0.43	×3.2 ± 0.61
PSAm	99.21 ± 0.10	98.31 ± 0.32	97.16 ± 0.19	×3.1 ± 0.74
PSMHR B	98.99 ± 0.26	98.41 ± 0.45	96.46 ± 0.52	×2.9 ± 0.93
PSMHR A	99.23 ± 0.11	98.44 ± 0.43	4.2 ± 2.31[a]	×1.8 ± 0.91

[a] The differences between PSMHR A and PSMHR B, PSMHR A and PSAm, and PSMHR A and TCPS are statistically significant: $p < 0.001$. The differences between all other data are not statistically significant.

AFM tip from the PSAm surface requires a significant force, as expected from the highly attractive interfacial force, as described above. Also, detachment is a single-step event, in that the tip is released abruptly from the surface, once the bending force exceeds the adhesion force between the tip and the surface. The other extreme is PSMHR A, where detachment requires virtually no force, because of the lack of significant interaction between the tip and the PSMHR A aqueous interface. Between the two extremes lies PSMHR B, where some force is required to withdraw the tip from contact with the surface, even if definitely smaller than that required for PSAm. Importantly, detachment is now a multistep event, as shown by the typical saw-tooth behavior of the retracting curve. This is more clearly shown in Figure 6b, which displays a greater detail of the same curve of Figure 6a. This behavior is generally accounted for by the stretching of polymeric segments[46] or, in general, by the tip winning its freedom from adhesive interactions with interacting species of different lengths. As stated in the experimental section, 72 curves for each sample were obtained. Adhesion interactions should be evaluated from a statistical point of view. A detailed quantitative study of forces operating at the aqueous interfaces of HR-coated PS is in progress and involves the use of surface-functionalized tips. For the sake of the present qualitative study, it is important to state that about 80% of the PSMHR B curves showed a behavior similar to that shown in Figure 6b.

Cell Adhesion Studies. Results of cell adhesion studies are shown in Tables 4 (L-929) and 5 (SMC). The two different polysaccharides had very significant effects on cell behavior, in particular, on cell adhesion and morphology. Trypan blue exclusion test showed that there was no significant difference in cell viability between poorly adherent and spread cells, thus, confirming that the observed results were not due to effects on cell health. The surface coated by long-haired MHR A is significantly less adhesive than the MHR B-coated surface, and this trend was observed with both continuous L-929 and primary SMC.

Figures 7 (a−d, L-929) and 8 (a−d, SMC) show the cell morphology on PSMHR B and PSMHR A after 3 and 24 h of culture. While cells are well spread and have a flat morphology on PSMHR B (completely similar to that observed on TCPS and PSAm), as a consequence of strong adhesion, they show a rounded morphology and a significant lower density on PSMHR A. In the latter case, the surface is definitely less adhesive toward cells (or more cell-resistant).

Discussion

Precise engineering of plant HR by enzymes offers interesting new opportunities in the surface modification of medical devices and materials by polysaccharides. In the present work, PS Petri dishes were surface modified by two different MHRs, prepared from apple pectin. The coupling reaction involves condensation between carboxyl groups of HR and amino groups introduced by plasma deposition on PS surfaces.

Surface characterization data confirmed the successful modification of the PS surface: in particular, XPS analysis shows an increase of the O/C and N/C ratios, with an overall surface composition consistent with previous reports on surface immobilization of polysaccharides.[8,37,38] In agreement with previous work and chemical sense, the thickness of the polysaccharide surface layer is, at least in a vacuum, thinner than the XPS sampling depth.

Water contact angle data indicate, both for PSMHR A and PSMHR B, that the high surface density of hydrogen-bonding moieties on the sample surfaces leads to strong interaction with water, as expected. Detailed analysis of contact angle data yields interesting information. The following simple model could be used, as a first approximation, to interpret the data of Table 3 and relevant statistical analysis: the advancing angle is typical of the low-energy portion of surface,[47] while the receding one reflects the high-energy portion. The equilibrium sessile angle is representative of the average character of the surface; the sessile angle is close to advancing and does not give further information.

PSMHR A is completely different from TCPS for all wettability parameters; it is indistinguishable from PSAm as far as the low-energy portion of the surface is concerned and indistinguishable from PSMHR B for the high-energy portion of the surface.

PSMHR B is indistinguishable from PSMHR A for the high-energy portion of the surface; however, upon increasing the vibration frequency and squeezing a water drop on the surface the material changes irreversibly, becoming on the average indistinguishable from PSMHR A, suggesting some dynamic properties of the surface (in the sense proposed by Andrade).[47]

AFM and cell adhesion data offer different and complementary views of forces operating at aqueous interfaces. Both experiments indicate that the two polysaccharides engender different interfacial fields of forces: immobilization of the short-haired MHR B yielded an aqueous interface that supports adhesion and spreading of both continuous L-929 fibroblasts and primary SMC. Force−separation curves
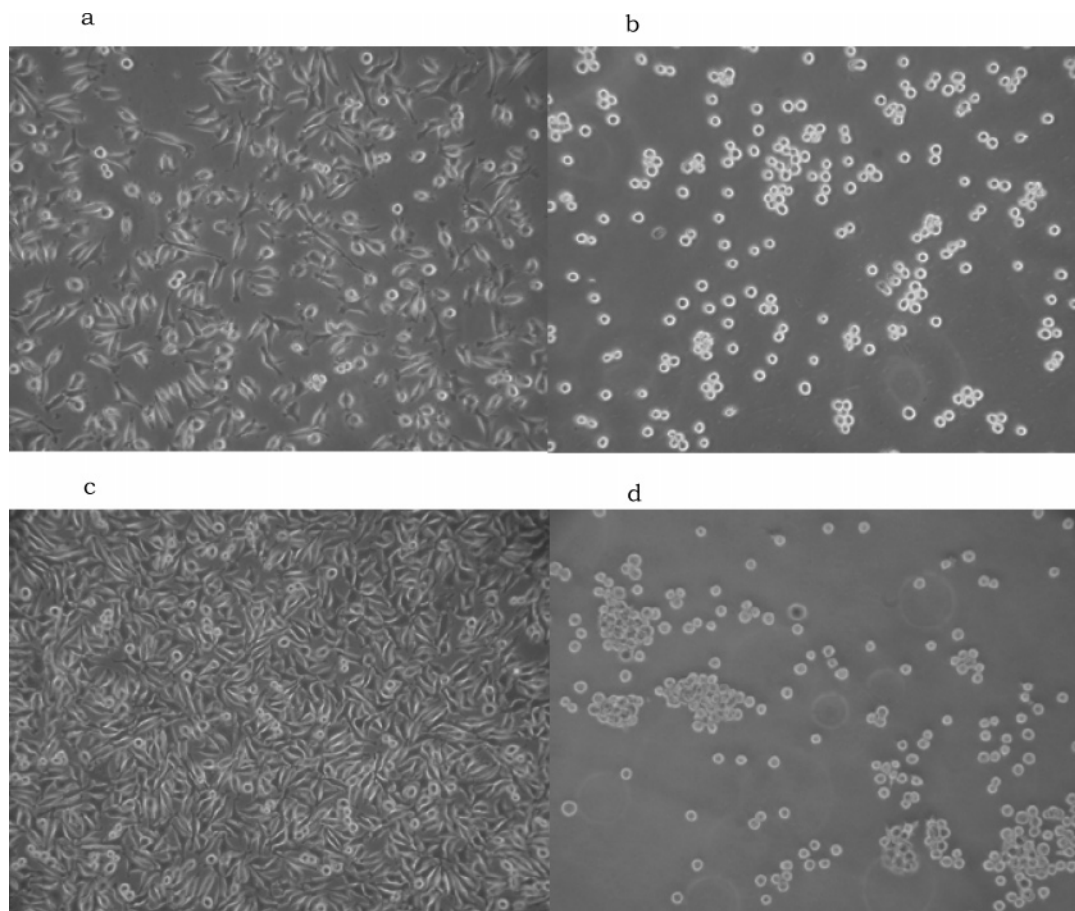
Figure 7. Inverted microscope photographs showing L-929 cell density and morphology after (a) 3 h on PSMHR B; (b) 3 h on PSMHR A; (c) 24 h on PSMHR B; and (d) 24 h on PSMHR A.

measured at the PSMHR B−saline interface show a comparatively short range of interactions, as compared to PSMHR A and other surface-immobilized polysaccharides. This is consistent with the proposed structure of the immobilized polysaccharides having short, neutral hairs. AFM data, in particular retraction curves (Figure 6), suggest that cell adhesion was, in this case, related to the polysaccharide layer and not, for instance, to incomplete masking by the polysaccharide of the underlying, highly cell-adhesive, aminated layer. Actually, retraction curves show that, even after the significant compression of the tip on the surface, which occurred in the last part of the approaching curve, the tip was interacting with polymeric segments and not with the aminated surface (Figure 6).

Contrary to MHR B, immobilized MHR A significantly reduced cell adhesion (Tables 4 and 5); also, the cell morphology reflected the diminished strength of the cell−surface interaction (Figures 7 and 8). The moderately cell-resistant character of PSMHR A can be accounted for by the decreased adsorption, from the culture medium, of proteins that promote cell adhesion. The retraction curve of PSMHR A (Figure 6) actually indicated a lack of significant interactions between the tip and the sample, suggesting a less-adhesive interface as compared to that of PSMHR B. The physical basis for this low-adhesion surface could be the steric-hydration force engendered by the long hairs of MHR A, analogous of what was observed and debated in the case of poly(ethylene oxide)-coated surfaces[48−52] and the

hydrogel-like nature of this interface. Cell morphology data of Figures 7 and 8 show the significant implications of the present approach to the surface modification of medical devices: it is generally accepted that, for a number of cell types, cell spreading promotes proliferation while a rounded cell shape is associated with a differentiated phenotype.[53−56] Actually, in a separate set of experiments, B16C3 nonmetastatic murine melanoma cells cultured on PSMHR A showed a nicely differentiated behavior (unpublished results). Thus, tailoring of the neutral side chain length could be a significant tool in directing a given cell type toward proliferation or differentiation. The observation that mammalian cell behavior can be directed by engineering plant components underlines the fascination and interest of the present approach.

Coming back to force−separation curves, as discussed by Butt and co-workers, the force upon approach on surfaces bearing "soft" polymer overlayers can be fitted by a simple exponential:[46]

$$F = A \exp(-D/\lambda) \tag{1}$$

where D is the tip−sample distance. The amplitude A and the typical decay length λ are the fitting parameters. It can be shown[46] that

$$\lambda = L_0/2\pi \tag{2}$$

where L_0 is the equilibrium thickness of the grafted polymer brush. Equation 2 is strictly valid only under a number of
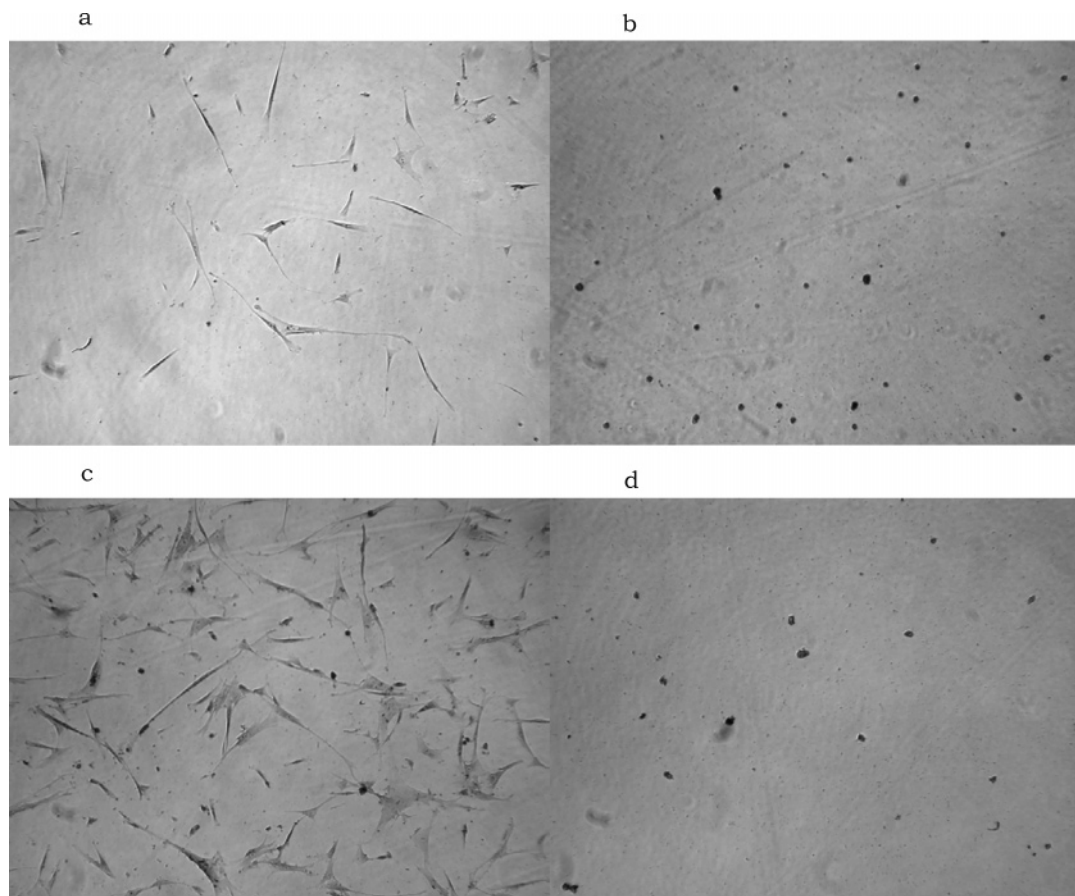
Figure 8. Inverted microscope photographs showing SMC cell density and morphology after (a) 3 h on PSMHR B; (b) 3 h on PSMHR A; (c) 24 h on PSMHR B; and (d) 24 h on PSMHR A.

assumptions, not all of them completely fulfilled in the present case. However, taking into full account all the limitations of this approach, it is of some interest to evaluate figures arising from the experimental curves. In particular, the repulsive force detected upon the approach of the tip to PSMHR B and PSMHR A yields reasonable exponential fits ($r^2 = 0.964$ for PSMHR B and 0.983 for PSMHR A), with calculated $\lambda = 2.1$ nm (PSMHR B) and 3.5 nm (PSMHR A). Using eq 2, it is then possible to calculate an equilibrium thickness of the polymer brush of 13.3 and 22.0 nm, respectively.

To compare present results with those obtained on related systems, it must be underlined that the present polysaccharide-coated surfaces, even in the case of long-haired MHR A, show a shorter range of repulsive interaction as compared to alginate- or hyaluronan-coupled surfaces.[2,40] In the latter case,[40] a decaying length of 7.1 nm was obtained for hyaluronan immobilized to an aminated substrate by carbodiimide condensation (the detected figure was apparently unaffected by the hyaluronan MW). These data could reflect an actual shorter range of interaction in the present case or a lower crowding of polysaccharide moieties at the interface (in this respect, it is noteworthy that the hyaluronan-coated surfaces referred to above were completely resistant to L-929 cell adhesion),[40] or the presently detected figures could be due either to a low density of neutral side chains (that is, to the frequency of side chains along the HR backbone), which could be not high enough to establish a true brush-like regime, or to the mechanical properties of the side chains

protruding in the aqueous solution, which could be too soft to be adequately handled by a tip having a force constant of 0.06 N/m. This is reasonable, because, contrary to heavily hydrogen-bonded alginate and hyaluronan, here we are dealing with neutral chains and other modifications (methyl and acetyl esterification) which may affect, for example, the ionic repulsion of the molecule. As reported above, an in depth study, involving functionalized tips and characterized by different force constants, is presently going on.

Conclusions

In conclusion, the data presented in this paper show that enzymatically MHR were covalently coupled to aminated surfaces and that the different nature of the HR side chains affect the interfacial field of forces and, as a consequence, cell adhesion behavior. In agreement with existing theories, the long-haired MHR A is more cell-resistant than the short haired MHR B. However, because the length of the side chains is not the only parameter varying between the two samples, other effects may play a role as well. In the case of MHR B, two widely different cell lines show a spread morphology and adhesion is quantitatively comparable to that observed on conventional TCPS. In the case of immobilized MHR A, cell density decreases significantly and cell morphology is rounded. Overall, these data show that engineering of plant pectins can be a valuable tool to prepare novel and finely tuned polysaccharides differing in charge, MW, degree of branching, and acetylation, to be used in the

surface modification of medical devices and materials. The growth of the understanding of the mechanisms that control the hydration, specific interactions, and bioactive behavior of these polysaccharides could promote an analogous growth of the understanding of the molecular structure−function relationships of polysaccharide-modified surfaces and devices. Further research will be directed to reveal the precise effect of the different structural elements of pectins and the level of methyl and acetyl esterification present on the behavior of the different cell lines used.

References and Notes

(1) Kim, S. H.; Hoshiba, T.; Akaike, T. *J. Biomed. Mater. Res.* **2003**, *67A*, 1351−1359.

(2) Morra, M.; Cassinelli, C. In *Water in Biomaterials Surface Science*; Morra, M., Ed.; Wiley: Chichester, 2001; pp 353−387.

(3) Larm, O.; Larsson, R.; Olsson, P. *Biomater., Med. Devices, Artif. Organs* **1983**, *11*, 161−169.

(4) Sanchez, J.; Elgue, G.; Riesenfeld, J.; Olsson, P. *J. Biomed. Mater. Res.* **1995**, *29*, 655−662.

(5) Lindhout, T.; Blezer, R.; Schoen, P.; Willems, G. M.; Fouache, B.; Verhoeven, M.; Hendriks, M.; Cahalan, L.; Cahalan, P. T. *J. Biomed. Mater. Res.* **1995**, *29*, 1255−1262.

(6) Blezer, R.; Fouache, B.; Willems, G. M.; Lindhout, T. *J. Biomed. Mater. Res.* **1997**, *37*, 108−114.

(7) Brink, C.; Osterberg, E.; Holmberg, K.; Tiberg, F. *Colloids Surf.* **1992**, *66*, 149−158.

(8) Osterberg, E.; Bergstrom, K.; Holmberg, K.; Schuman, T. P.; Riggs, J. A.; Burns, N. L.; Van Alstine, J. M.; Harris, J. M. *J. Biomed. Mater. Res.* **1995**, *29*, 741−753.

(9) Frazier, R. A.; Matthijs, G.; Davies, M. C.; Roberts, C. J.; Schacht, E.; Tendler, S. J. B. *Biomaterials* **2000**, *21*, 957−966.

(10) *The Biology of Hyaluronan*; Evered, D., Whelan, J., Eds.; Wiley: Chichester, 1989.

(11) *The Chemistry, Biology and Medical Applications of Hyaluronan and its Derivatives*; Laurent, T. C., Ed.; Portland Press, Ltd.: London, 1998.

(12) *Redefining Hyaluronan;* Abatangelo, G., Weigel, P. H., Eds.; Elsevier: Amsterdam, 2000.

(13) Moore, K. In *Hyaluronan*; Kennedy, J. F., Phillips, G. O., Williams, P. A., Hascall, V. C., Eds.; Woodhead Publishing, Ltd.: Cambridge, 2002; Vol. 2, pp 137−146.

(14) Chen, W. Y. J. In *Hyaluronan*; Kennedy, J. F., Phillips, G. O., Williams, P. A., Hascall, V. C., Eds.; Woodhead Publishing, Ltd.: Cambridge, 2002; Vol. 2, pp 147−156.

(15) Qin, Y.; Gilding, G. K. *Med. Dev. Technol.* **1996**, *7*, 32−39.

(16) Sayag, J.; Meaume, S.; Bohbot, S. *J. Wound Care* **1997**, *5*, 357−362.

(17) Schols, H. A.; Voragen, A. G. J. In *Pectins and their Manipulation*; Seymour, G. B., Knox, J. P., Eds.; Blackwell: Oxford, 2003; pp 1−29.

(18) Ridley, B. L.; O'Neill, M. A.; Mohnen, D. *Phytochemistry* **1999**, *57*, 929−967.

(19) Voragen, A. G. J.; Pilnik, W.; Thibault, J.-F.; Axelos, M. A. V.; Renard, C. M. G. C. In *Food polysaccharides and their applications*; Stephen, A. M., Ed.; Marcel Dekker, Inc.: New York, 1995; pp 287−339.

(20) Schols, H. A.; Bakx, E. J.; Schipper, D.; Voragen, A. G. J. *Carbohydr. Res.* **1995**, *279*, 265−279.

(21) Schols, H. A.; Voragen, A. G. J. In *Progress in Biotechnology 14: Pectins and pectinases*, Proceedings of an Int. Symp., Wageningen, The Netherlands, 1995; Visser, J., Voragen, A. G. J., Eds.; Elsevier: Amsterdam, The Netherlands, 1996; pp 3−19.

(22) Vincken, J. P.; Schols, H. A.; Oomen, R. J. F. J.; McCann, M. C.; Ulvskov, P.; Voragen, A. G. J.; Visser, R. G. F. *Plant Physiol.* **2003**, *132*, 1781−1789.

(23) Oomen, R. J. F. J.; Vincken, J. P.; Bush, M. S.; Skjøt, M.; Doeswijk-Voragen, C. H. L.; Ulvskov, P.; Voragen, A. G. J.; McCann, M. C.; Visser, R. G. F. In *Advances in pectin and pectinase research*; Visser, R. G. F., Schols, H. A., Voragen, A. G. J., Eds.; Kluwer Academic Publishers: Dordrecht, The Netherlands, 2003; pp 15−34.

(24) McCann, M.; Bush, M.; Milioni, D.; Sado, P.; Stacey, N. J.; Catchpole, G.; Defernez, M.; Carpita, N. C.; Höfte, H.; Ulvskov, P.; Wilson, R. H.; Roberts, K. *Phytochemistry* **2001**, *57*, 811−821.

(25) Schols, H. A.; Voragen, A. G. J. *Carbohydr. Res.* **1994**, *256*, 83−95.

(26) Schols, H. A.; Posthumus, M. A.; Voragen, A. G. J. *Carbohydr. Res.* **1990**, *206*, 117−129.

(27) Wagner, H.; Kraus, S. In *Bioactive Carbohydrate Polymers*; Paulsen, B. S., Ed.; Kluwer Academic Publishers: Dordrecht, The Netherlands, 2000; pp 1−14.

(28) Yamada, H. In *Bioactive Carbohydrate Polymers*; Paulsen, B. S., Ed.; Kluwer Academic Publishers: Dordrecht, The Netherlands, 2000; pp 15−24.

(29) Nangia-Makker, P.; Conklin, J.; Hogan, V.; Raz, A. *Trends Mol. Med.* **2002**, *8*, 187−192.

(30) Della Volpe, C.; Maniglio, D.; Siboni, S.; Morra, M. *Oil Gas Sci. Technol.* **2001**, *56*, 9−22.

(31) Della Volpe, C.; Maniglio, D.; Morra, M.; Siboni, S. *Colloids Surf., A* **2002**, *6*, 46−67.

(32) Della Volpe, C.; Brugnara, M.; Maniglio, D.; Siboni, S.; Wangdu, T. Presented at the IV Congress on Contact angles, Wettability and Adhesion, Philadelphia, PA, 23−25 June, 2004.

(33) Schols, H. A.; Geraeds, C. C. J. M.; Leeuwen, M. F. S. v.; Kormelink, F. J. M.; Voragen, A. G. J. *Carbohydr. Res.* **1990**, *206*, 105−115.

(34) Gombotz, A. G. J.; Hoffman, A. S. *J. Appl. Polym. Sci., Appl. Polym. Symp.* **1988**, *42*, 285−303.

(35) Puleo, D. A.; Kissling, R. A.; Sheu, M. S. *Biomaterials* **2002**, *23*, 2079−2087.

(36) Han, L. M.; Timmons, R. B. *J. Polym. Sci., Part A: Polym. Chem.* **1998**, *36*, 3121−3129.

(37) Morra, M.; Cassinelli, C. *Surf. Interface Anal.* **1998**, *26*, 742−751.

(38) Morra, M.; Cassinelli, C. *J. Biomater. Sci., Polym. Ed.* **1999**, *10*, 1107−1124.

(39) Andrade, J. D.; King, R. N.; Gregonis, D. E.; Coleman, D. L. *J. Polym. Sci.: Polym. Symp.* **1979**, *66*, 313−336.

(40) Morra, M.; Cassinelli, C.; Pavesio, A.; Renier, D. *J. Colloid Interface Sci.* **2003**, *259*, 236−243.

(41) Dupont-Gillaine, C. C.; Nysten, B.; Hlady, V.; Rouxhet, P. G. *J. Colloid Interface Sci.* **1999**, *220*, 163−171.

(42) Vogler, E. A. *Adv. Colloid Interface Sci.* **1998**, *74*, 69−95.

(43) Vogler, E. A. *J. Biomat. Sci., Polym. Ed.* **1999**, *10*, 1015−1046.

(44) Besseling, N. A. M. *Langmuir* **1997**, *13*, 2109−2116.

(45) Kurutz, J. W.; Xu, S. *Langmuir* **2001**, *17*, 7323−7332.

(46) Butt, H. J.; Kappl, M.; Mueller, H.; Raiteri, R.; Meyer, W.; Ruhe, J. *Langmuir* **1999**, *15*, 2559−2568.

(47) *Polymer Surface Dynamics*; Andrade, J. D., Ed.; Plenum Press: New York, 1988.

(48) *Poly(ethylene glycol): Chemistry and Biological Applications*; Harris, J. M., Zalipsky, S., Eds.; American Chemical Society: Washington, DC, 1997.

(49) Leckband, D.; Sheth, S.; Halperin, A. *J. Biomater. Sci., Polym. Ed.* **1999**, *10*, 1125−1148.

(50) Malmsten, M.; Lassen, B.; Holmberg, K.; Thomas, V.; Quash, G. *J. Colloid Interface Sci.* **1996**, *177*, 70−83.

(51) Szleifer, I. *Biophys. J.* **1997**, *72*, 595−608.

(52) Morra, M. In *Water in Biomaterials Surface Science*; Morra, M., Ed.; Wiley: New York, 2001; pp 307−332.

(53) Boudreau, N. J.; Jones, P. L. *Biochem. J.* **1999**, *339*, 481−488.

(54) Sieminski, A. L.; Gooch, K. J. *Biomaterials* **2000**, *21*, 2233−2241.

(55) Dike, L. E.; Chen, C. S.; Mrksich, M.; Tien, J.; Whitesides, G. M.; Ingber, D. E. *In Vitro Cell Dev. Biol. Anim.* **1999**, *35*, 441−448.

(56) Chen, C. S.; Alonso, J. L.; Ostuni, E.; Whitesides, G. M.; Ingber, D. E. *Biochem. Biophys. Res. Commun.* **2003**, *307*, 355−361.